Electronic Supplementary Material (ESI) for Journal of Materials Chemistry A.
This journal is © The Royal Society of Chemistry 2022

Supporting Information

Linear 2D-conjugated Polymer Based on 4,8-Bis(4-chloro-5-tripropylsilyl-thiophen-2-yl)benzo[1,2-b:4,5-b']dithiophene (BDT-T-SiCl) for Low Voltage Loss Organic Photovoltaics

Jialing Zhou[1,2], Peng Lei[1, 2], Yanfang Geng[*1, 2], Zehua He[1, 3], Xianda Li[1, 3], Qingdao Zeng[1], Ailing Tang[1], Erjun Zhou*[*1, 2]*

[1] CAS Key Laboratory of Nanosystem and Hierarchical Fabrication, CAS Center for Excellence in Nanoscience, National Center for Nanoscience and Technology, Beijing 100190, China.

[2] Center of Materials Science and Optoelectronics Engineering, University of Chinese Academy of Sciences, Beijing 100049, China.

[3] Henan Institutes of Advanced Technology, Zhengzhou University, Zhengzhou 450003, China.

E-mail: gengyf@nanoctr.cn; zhouej@nanoctr.cn

Materials and Synthesis

The monomer 4 was synthesized according to the literature [1], **monomer 1**, **2** and **5** were purchased from Solarmer.

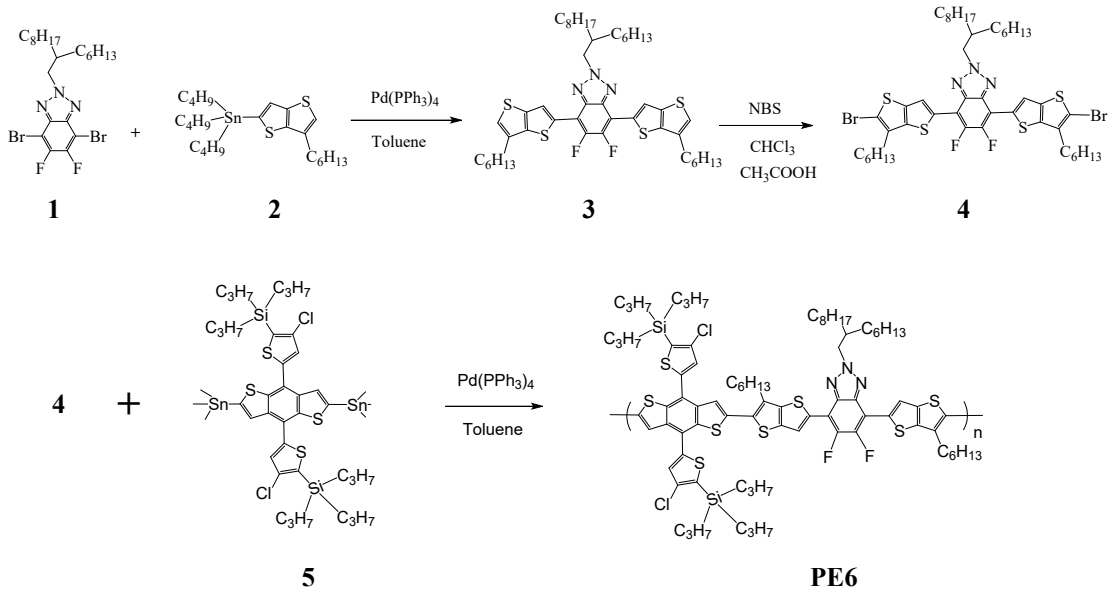

1 **2** **3** **4**

4 + **5** → **PE6**

Scheme S1. Synthetic route of polymer **PE6**.

Synthesis of compound (3)

Compound 1 (3.0 g, 5.47 mmol), **compound 2** (6.2 g, 12.04 mmol) and $Pd(PPh_3)_4$ (70 mg) were dissolved in toluene (40 mL). The mixture was refluxed at 110℃ for 48h under the protection of nitrogen, then allowed to cool to room temperature. Water (100 mL) was added and the mixture was extracted with $CHCl_3$ (3×100 mL). The organic phase was dried over anhydrous $MgSO_4$. After removing the solvent, the residue was purified by column chromatography on silica gel (petroleum ether: dichloromethane = 15:1 as the eluent). **Compound 3** was obtained as a yellow solid. Yield: 4.2 g (93%). ^{1}H NMR (400 MHz, $CDCl_3$) δ 8.53 (s, 2H), 7.06 (s, 2H), 4.75 (d, J = 6.5 Hz, 2H), 2.78 (t, J = 7.6 Hz, 4H), 2.31 (m, 1H), 1.88 – 1.71 (m, 4H), 1.46 – 1.19 (m, 36H), 0.95 – 0.81 (m, 12H).

Synthesis of compound (4)

Compound 3 (4.2 g, 5.1 mmol) was dissolved in the mixture of $CHCl_3$ (80 mL) and acetic acid (80 mL) in the absence of light. NBS (2.0 g, 11.2 mmol) was added in

portions at room temperature, and then the mixture stirred for 12 h. Water (200 mL) was added and the mixture was extracted with $CHCl_3$ (3×200 mL), The organic phase was dried over anhydrous $MgSO_4$. After removing the solvent, the crude product was further purified by column chromatography on silica gel (petroleum ether: dichloromethane = 20:1 as the eluent) and **compound 4** was obtained as a yellow solid. Yield: 4.2 g (84%). ^{1}H NMR (400 MHz, $CDCl_3$) δ 8.57 – 8.30 (m, 2H), 4.75 (d, J = 6.5 Hz, 2H), 2.79 (t, J = 7.6 Hz, 4H), 2.31 (m, 1H), 1.92 – 1.64 (m, 4H), 1.50 – 1.13 (m, 36H), 0.87 (m, 12H).

Synthesis of polymers PE6

Compound 4 (245.5 mg, 0.25 mmol) and **compound 5** (265.4 mg, 0.25 mmol) were dissolved in toluene (15 mL, with sodium reflux) with a 100 mL Schlenk flask, under the protection of nitrogen. Then $Pd(PPh_3)_4$ (14.4 mg) was added as catalyst, and the mixture was purged by nitrogen for another 15 min. After that, the mixture was starred at 110 °C for 48 h. Then allowed to cool to room temperature the mixture was precipitated into methanol. The raw polymer was put in Soxhlet extraction and extracted with methanol, hexane, dichloromethane and chloroform. The chloroform fraction was precipitated in methanol, dried under vacuum at 50 °C overnight, polymer **PE6** was obtained as a crimson solid (127 mg, 47% yield). Mn = 42.2 kDa, Mw = 122.5 kDa, PDI = 2.90).

Measurements and characterizations

Molecular weight of the polymer was measured on Angilent Technologies PL-GPC 220 high-temperature-chromatograph at 150 °C using a calibration curve of polystyrene standards. UV–vis spectra were conducted with Lambda-950 (Perkin Elmer Instruments Co. Ltd., America). Cyclic voltammetry (CV) measurements were carried out using an electrochemical workstation, equipped with a standard three-electrode configuration. Typically, a three-electrode cell equipped with Pt plate which coated with a thin film as working electrode, an Ag/AgCl (0.01 M in anhydrous acetonitrile) reference electrode, and a Pt wire counter electrode was employed. The measurements were done in

anhydrous acetonitrile with tetrabutylammonium hexafluorophosphate (0.1 M) as the supporting electrolyte under an argon atmosphere at a scan rate of 100 Mv/s. The potential of Ag/AgCl reference electrode was internally calibrated by using the ferrocene/ferrocenium redox couple (Fc/Fc^+).

The *J*−*V* curves were measured in glove box with a Keithley 2420 source measure unit. The photocurrent was obtained under illumination using an Oriel Newport 150W solar simulator (AM 1.5G), and the light intensity was calibrated with a Newport reference detector (Oriel PN 91150 V). The EQE measurements of the devices were performed in air with an Oriel Newport system (Model 66902). Two-dimensional grazing incidence wide angle X-ray scattering (2D-GIXD) analyses were measured at the XEUSS SAXS/WAXS equipment. The data were obtained with an area Pilatus 100k detector with a resolution of 195 × 487 pixels (0.172 mm × 0.172 mm). The X-ray wavelength was 1.54 Å, and the incidence angle was 0.2°. The samples were spin-coated onto the PEDOT: PSS/Si substrate using the optimized device fabrication conditions. AFM images were obtained on a Multimode 8 in tapping mode. TEM images were measured with Tecnai G2 F20 U-TWIN (FEI) operated at 200 Kv. The TEM specimens were prepared by transferring the spin-coated films to the 200 mesh copper grids. The thickness of the active layer was tested on a Kla-TencorAlpha-StepD-120 Stylus Profiler. FTPS-EQE measurements were carried out by an integrated system (PECT600, Enlitech). EL measurements were carried out by applying external voltage/current sources through the devices (REPS, Enlitech). The voltage loss is calculated by software SQ-VLA (Enlitech).

Photovoltaic device fabrication

The OSCs devices were fabricated with a conventional structure of ITO/PEDOT: PSS/active layer/ PDINO or PFN-Br /Al. A thin layer of PEDOT: PSS (30 nm, Baytron PH1000) was spin-casted on pre-cleaned ITO-coated glass at 3000 rpm. After baking at 150 °C for 15 min, the substrates were transferred into glovebox. Optimized devices

were prepared under the following conditions. The Donor: Acceptor (D: A) ratio of 1:1.5 (w/w) for **PE6: Y6** and **PE6: IT-M** was dissolved in chloroform (CF) with a total concentration of 16 mg/mL and stirred for 1 hour at 48 °C. Then, the active layer was spin-coated (2000 rpm) from the above solution with thermal annealing at 90 ℃ for 10 min. PDINO as cathode interface layer (CIL) was spin-coated on the top of active layer at 3000 rpm for 30 s, which was dissolved in methanol at a concentration of 1.0 mg/ mL. For **PE6: BTA3** combination, the D: A ratio of 1:1 (w/w) was dissolved in CF with a total concentration of 14 mg/ mL and stirred for 1 hour at 48 °C. Then, the active layer was spin-coated (3000 rpm) from the above solution with thermal annealing at 150 ℃, 10 min. A PFN-Br layer was spin-coated on the top of all the active layers at 3000 rpm for 30 s, which was dissolved in methanol at a concentration of 0.5 mg/mL. Finally, an Al (80 nm) metal top electrode was thermal evaporated onto the active layer under about 4×10^{-4} Pa. The active area of the device was 0.04 cm^2 defined by shadow mask. The thickness of the active layer for **PE6: Y6**, **PE6: IT-M** and **PE6: BTA3** are estimated to be 131, 130 and 162 nm, respectively.

Carrier mobility measurements

The carrier mobilities of the polymer was investigated by the space charge limited current (SCLC) method. The hole mobility of the blend films was measured with the device structure of ITO/PEDOT: PSS/active layer (~100 nm)/Au (80 nm) while the electron mobility of the blends was measured with the device structure of ITO/TIPD/active layer (~100 nm)/Al (80 nm). The SCLC model is described by modified Mott-Gurney law:

$$J = (9/8)\ \varepsilon_0\varepsilon_r\mu\ (V^2/L^3)$$

where J stands for current density, ε_0 is the permittivity of free space, ε_r is the relative dielectric constant of the transport medium, which is assumed to be around 3 for the conjugated polymers, μ is the carrier mobility, V is the internal potential in the device and L is the film thickness of the active layer.

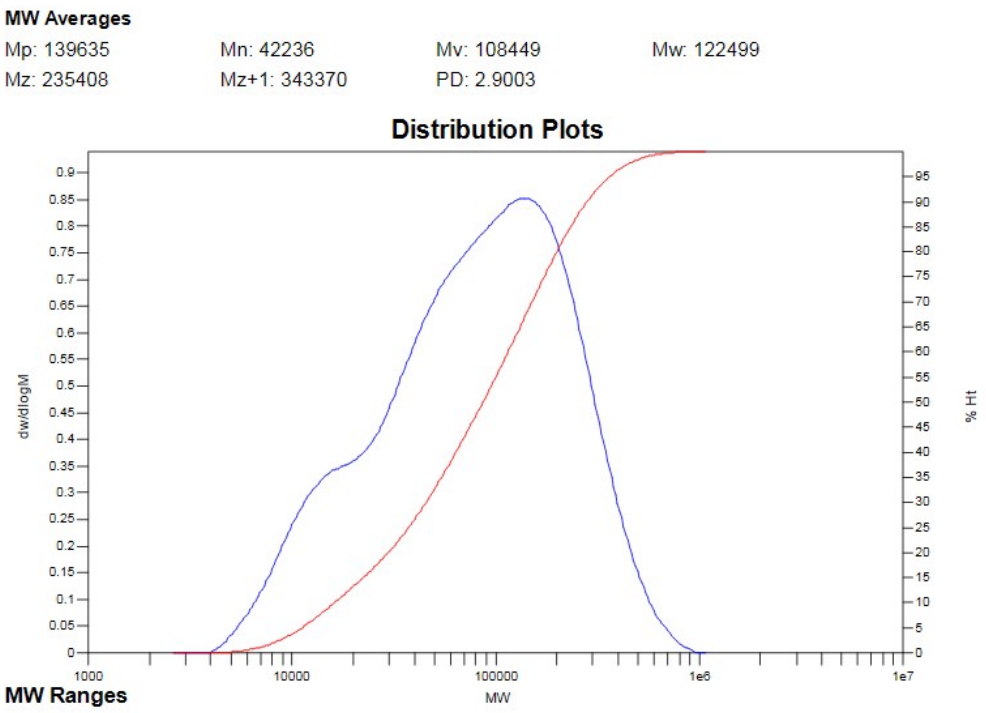

Figure S1. The gel permeation chromatography (GPC) measurement of **PE6.**

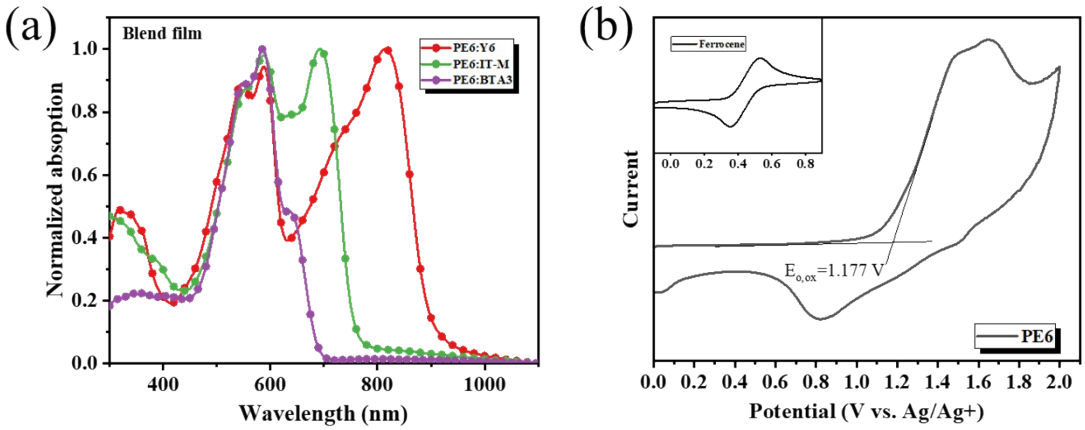

Figure S2. (a) UV-vis absorption spectra of three blend film; (b) Cyclic voltammograms of **PE6** with Ag/AgCl as a reference electrode

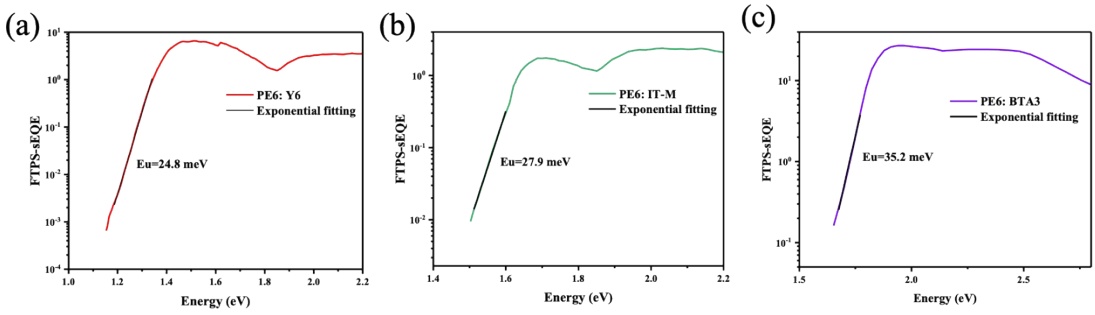

Figure S3. FTPS-EQE spectra of the three devices.

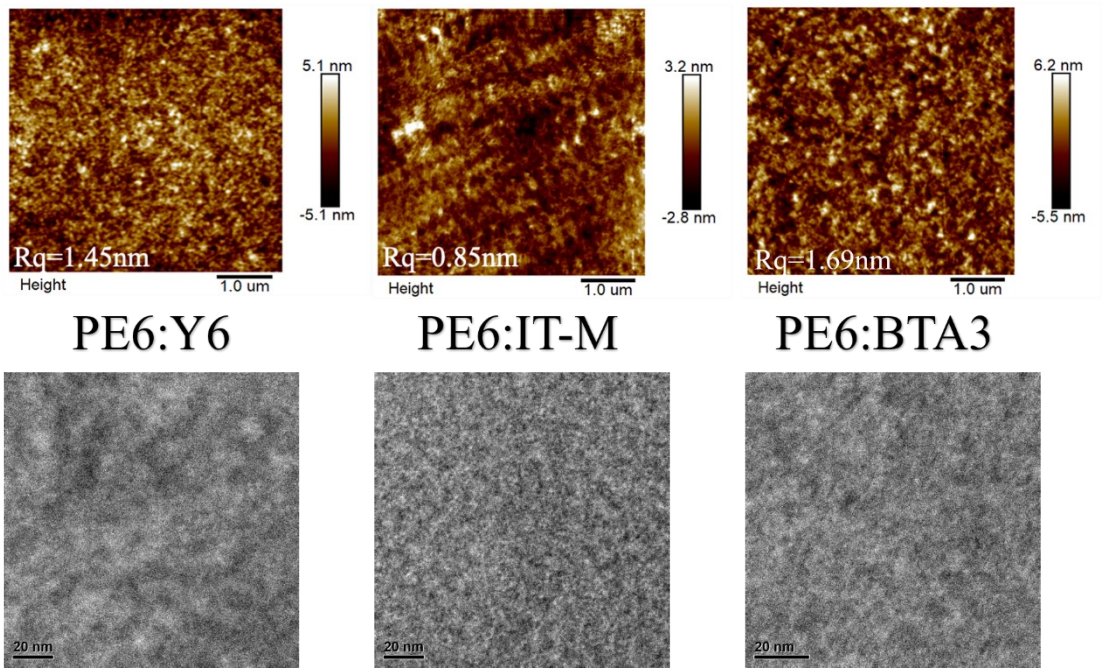

Figure S4. AFM height images (top) and TEM images (bottom) of **LP6:** NFA blend films.

Table S1. *V*oc, *J*sc, FF, PCE for various BTA-polymer NFA solar cells（V_{OC}＞1V or PCE＞12%）.

Polymer: Non-Fullerene	*V*oc (V)	*J*sc (mA·cm^{-2})	FF(%)	PCE (%)	Ref.
PvBDTTAZ :O-IDTBR	1.08	16.26	63.6	11.6	2
PIDT-DTffBTA:BTA3	1.21	8.68	54.0	5.67	3
PfBTAZ:O-IDTBR	1.00	11.70	64.0	7.50	4
J71:m-ITIC	0.94	18.09	70.6	12.05	5
FTAZ-IDIC	0.85	21.58	71.0	13.03	6
FTAZ:IDIC	0.84	20.80	71.8	12.50	7
J71:ITIC5	0.89	18.35	74.7	12.20	8
PTBD-BZ:TBDB-PNa	0.91	19.61	70.2	12.47	9
L610:IT-4F	0.79	20.76	73.5	12.10	10
J11:m-ITIC	0.94	18.05	73.0	12.32	11
J71:ITC6-IC	0.98	18.57	66.4	12.08	12
J101:ITIC	0.95	17.70	73.7	12.47	13
J101:ZITI	0.94	21.25	72.5	14.43	
PBZ-ClSi:IT-4F	0.93	19.20	71.5	12.80	14
PSS2: EH-IDTBR	1.07	14.12	53.5	8.05	15
PBDD-BTZ-3:ITIC-Th	1.07	11.90	56.7	7.30	16
J11:Y10	0.89	21.21	71.6	13.46	17
PBDB-TAZ20:ITIC	0.87	19.03	73.5	12.02	18
PBDTTz-SBP:ITIC	0.91	18.52	71.4	12.09	19
PBTA-TF:ITCC	1.00	15.54	67.0	10.40	20
PBTA-TF:IT-M	0.97	17.76	71.0	12.20	
PBTA-TF:IT-4F	0.96	18.71	70.0	13.10	
J61:BTA3	1.15	10.84	66.0	8.25	1
PE1:BTA3	1.11	11.95	64.0	8.43	
PE2:BTA3	1.26	8.06	57.0	5.83	
PBDTSF-TZNT:IT-4F	0.93	19.23	74.1	13.25	21
PBDTFBTA-TSi:Y6	0.77	24.63	74.8	14.18	22
PT-68:ITIC	1.02	11.49	46.1	5.39	23
PT-810-H:ITIC	1.04	12.43	53.1	6.91	
PT-810-I:ITIC	1.04	10.30	55.9	5.99	
J52:BTA3	1.07	14.62	60.3	9.41	24
J52-Cl:BTA3	1.24	13.16	66.6	10.50	
J52-Cl:Y6	0.84	23.77	61.4	12.31	25
PE4:Y6	0.84	22.21	75.4	14.02	
PE44:Y6	0.82	25.29	66.0	13.62	26
PE5:Y6	0.84	24.98	69.1	14.48	27
PE5-Cl:Y6	0.86	24.24	67.3	13.41	
PE51:Y6	0.79	24.11	69.8	13.34	28
PE52:Y6	0.80	25.36	71.9	14.61	

PE53:Y6	0.83	23.64	69.8	13.72	
PE31:BTA5	1.11	13.68	66.4	10.08	29
PE32:BTA5	1.10	11.65	57.7	7.40	
PE33:BTA5	1.16	12.68	61.1	8.99	
J52-Cl:BTA5	1.21	11.36	62.9	8.64	
J52-Cl:F-BTA3	1.15	12.81	68.6	10.10	30
F11:F-BTA3	1.12	13.00	69.0	10.04	
PE52:F-BTA3	1.14	10.53	56.5	6.78	
PE25:BTA3	1.22	11.53	64.6	9.08	31
PE25:F-BTA3	1.13	12.81	72.4	10.48	
PE25:Cl-BTA3	1.09	13.65	72.3	10.75	
J71:BTA3	1.20	10.39	69.0	8.60	32
PBTA-PSF:ITIC	1.01	18.51	74.4	13.91	33

Table S2. Photophysical properties and energy levels of polymers.

Polymer	**Film λ_{max} (nm)**	**ε (M^{-1} cm^{-1})**	**Film λ_{edge} (nm)**	**E_g^{opt} (eV)**	**LUMO[a] (eV)**	**HOMO (eV)**
PE6	544, 582	8.41×10^4	630	1.98	-3.55	-5.53
PE4	547, 595	7.81×10^4	634	1.96	-3.49	-5.42

[a] $E_{LUMO} = E_{HOMO} + E_g^{opt}$

Table S3. Photovoltaic performance of **PE6**-based OPV devices blending with other non-fullerenes.

Nonfullerene	*V*oc (V)	*J*sc (mA·cm^{-2})	FF(%)	PCE (%)
BTP-eC9	0.862	24.24	65.57	13.70
Y6-1O	0.899	21.18	70.47	13.44
IT-4F	0.899	18.52	61.30	10.21
F-BTA3	1.226	11.41	56.05	7.83

Table S4. In-plane (100) and out-of-plane (010) peaks, lamellar spacing (d) and π-π distance ($d_{\pi\text{-}\pi}$). The full width at half maximum (FWHM) of (100) peak is obtained by

fitting the corresponding curves. Coherence length is estimated by 2πK/FWHM, where the Scherrer constant K is 1.

Films	Out-of-plane				
	(100) ($Å^{-1}$)	d (Å)	(010) ($Å^{-1}$)	$d_{\pi-\pi}$ (Å)	Coherence length (Å)
PE6:Y6	0.299	21.01	1.74	3.61	21.03
PE6:IT-M	0.315	19.94	1.70	3.70	10.19
PE6:BTA3	0.327	19.21	1.73	3.63	12.65

References

1. Y. Chen, Q. Zhang, M. Du, G. Li, Z. Li, H. Huang, Y. Geng, X. Zhang and E. Zhou, *ACS Appl. Polym. Mater.*, 2019, **1**, 906-913.
2. S. Chen, Y. Liu, L. Zhang, P. C. Y. Chow, Z. Wang, G. Zhang, W. Ma and H. Yan, *J. Am. Chem. Soc.*, 2017, **139**, 6298-6301.
3. A. Tang, F. Chen, B. Xiao, J. Yang, J. Li, X. Wang and E. Zhou, *Front. Chem.*, 2018, **6**, 147.
4. S. Chen, L. Zhang, C. Ma, D. Meng, J. Zhang, G. Zhang, Z. Li, P. C. Y. Chow, W. Ma, Z. Wang, K. S. Wong, H. Ade and H. Yan, *Adv. Energy Mater.*, 2018, **8**, 1702427.
5. H. Bin, Y. Yang, Z. Peng, L. Ye, J. Yao, L. Zhong, C. Sun, L. Gao, H. Huang, X. Li, B. Qiu, L. Xue, Z.-G. Zhang, H. Ade and Y. Li, *Adv. Energy Mater.*, 2018, **8**, 1702324.
6. A. Mahmood, J. Hu, A. Tang, F. Chen, X. Wang and E. Zhou, *Dyes Pigments*, 2018, **149**, 470-474.
7. Y. Lin, F. Zhao, S. K. K. Prasad, J. D. Chen, W. Cai, Q. Zhang, K. Chen, Y. Wu, W. Ma, F. Gao, J. X. Tang, C. Wang, W. You, J. M. Hodgkiss and X. Zhan, *Adv. Mater.*, 2018, **30**, 1706363.
8. C. Yan, W. Wang, T.-K. Lau, K. Li, J. Wang, K. Liu, X. Lu and X. Zhan, *J. Mater. Chem. A.*, 2018, **6**, 16638-16644.
9. X. Wang, J. Han, H. Jiang, Z. Liu, Y. Li, C. Yang, D. Yu, X. Bao and R. Yang, *ACS Appl. Mater. Interfaces*, 2019, **11**, 44501-44512.
10. Z. Liao, Y. Xie, L. Chen, Y. Tan, S. Huang, Y. An, H. S. Ryu, X. Meng, X. Liao, B. Huang, Q. Xie, H. Y. Woo, Y. Sun and Y. Chen, *Adv. Funct Mater.*, 2019, **29**, 1808828.
11. B. Qiu, S. Chen, H. Li, Z. Luo, J. Yao, C. Sun, X. Li, L. Xue, Z.-G. Zhang, C. Yang and Y. Li, *Chem. Mater.*, 2019, **31**, 6558-6567.
12. R. Sun, J. Guo, C. Sun, T. Wang, Z. Luo, Z. Zhang, X. Jiao, W. Tang, C. Yang, Y. Li and J. Min, *Energy Environ. Sci.*, 2019, **12**, 384-395.
13. T. Wang, R. Sun, S. Xu, J. Guo, W. Wang, J. Guo, X. Jiao, J. Wang, S. Jia, X.

Zhu, Y. Li and J. Min, *J. Mater. Chem. A.*, 2019, **7**, 14070-14078.
14. W. Su, G. Li, Q. Fan, Q. Zhu, X. Guo, J. Chen, J. Wu, W. Ma, M. Zhang and Y. Li, *J. Mater. Chem. A.*, 2019, **7**, 2351-2359.
15. Q. Tu, C. Tang and Q. Zheng, *J. Mater. Chem. A.*, 2019, **7**, 3307-3316.
16. H. Guo, L. Chen, B. Huang, Q. Xie, S. Ding and Y. Chen, *Polym. Chem.*, 2019, **10**, 6227-6235.
17. Y. Zhang, F. Cai, J. Yuan, Q. Wei, L. Zhou, B. Qiu, Y. Hu, Y. Li, H. Peng and Y. Zou, *Phys. Chem. Chem. Phys.*, 2019, **21**, 26557-26563.
18. Y. Zhang, Y. Shao, Z. Wei, L. Zhang, Y. Hu, L. Chen, S. Chen, Z. Yuan and Y. Chen, *ACS Appl. Mater. Interfaces*, 2020, **12**, 20741-20749.
19. Y. Gao, Z. Wang, J. Zhang, H. Zhang, K. Lu, F. Guo, Z. Wei, Y. Yang, L. Zhao and Y. Zhang, *Macromolecules.*, 2018, **51**, 2498-2505.
20. W. Zhao, S. Zhang, Y. Zhang, S. Li, X. Liu, C. He, Z. Zheng and J. Hou, *Adv. Mater.*, 2018, **30**, 1704837.
21. K. Feng, J. Yuan, Z. Bi, W. Ma, X. Xu, G. Zhang and Q. Peng, *iScience*, 2019, **12**, 1-12.
22. Z. Tang, X. Xu, R. Li, L. Yu, L. Meng, Y. Wang, Y. Li and Q. Peng, *ACS Appl. Mater. Interfaces*, 2020, **12**, 17760-17768.
23. S. Ma, Y. Song, Z. Wang, B. He, X. Yang, L. Li, B. Xu, J. Zhang, F. Huang and Y. Cao, *Polymer*, 2019, **179**, 121580.
24. A. Tang, W. Song, B. Xiao, J. Guo, J. Min, Z. Ge, J. Zhang, Z. Wei and E. Zhou, *Chem. Mater.*, 2019, **31**, 3941-3947.
25. A. Tang, Q. Zhang, M. Du, G. Li, Y.-f. Geng, J. Zhang, Z. Wei, X. Sun and E. Zhou, *Macromolecules.*, 2019, **52**, 6227-6233.
26. P. Lei, B. Zhang, Y. Chen, Y. Geng, Q. Zeng, A. Tang and E. Zhou, *ACS Appl. Mater. Interfaces*, 2020, **12**, 38451-38459.
27. J. Zhou, P. Cong, L. Chen, B. Zhang, Y. Geng, A. Tang and E. Zhou, *J. Energy Chem.*, 2021, **62**, 532-537.
28. J. Zhou, B. Zhang, M. Du, T. Dai, A. Tang, Q. Guo and E. Zhou, *Nanotechnology*, 2021, DOI: 10.1088/1361-6528/abe896, 225403.
29. T. Dai, P. Lei, B. Zhang, A. Tang, Y. Geng, Q. Zeng and E. Zhou, *ACS Appl. Mater. Interfaces*, 2021, **13**, 21556-21564.
30. T. Dai, P. Lei, B. Zhang, J. Zhou, A. Tang, Y. Geng, Q. Zeng and E. Zhou, *ACS Appl. Mater. Interfaces*, 2021, **13**, 30756-30765.
31. T. Dai, Q. Nie, P. Lei, B. Zhang, J. Zhou, A. Tang, H. Wang, Q. Zeng and E. Zhou, *ACS Appl. Mater. Interfaces*, 2021, **13**, 58994-59005.
32. B. Xiao, Y. Geng, A. Tang, X. Wang, Y. Chen, Q. Zeng and E. Zhou, *Sol. RRL*, 2019, **3**, 1800332.
33. X. Li, G. Huang, N. Zheng, Y. Li, X. Kang, S. Qiao, H. Jiang, W. Chen and R. Yang, *Sol. RRL*, 2019, **3**, 1900005.